Polymer 79 (2015) 255–261

Contents lists available at ScienceDirect

Polymer

journal homepage: www.elsevier.com/locate/polymer

Water soluble, biodegradable amphiphilic polymeric nanoparticles and the molecular environment of hydrophobic encapsulates: Consistency between simulation and experiment

Robert D. Miller*, Rosmadi M. Yusoff [1], William C. Swope, Julia E. Rice, Amber C. Carr [2], Amanda J. Parker [3], Joseph Sly [4], Eric A. Appel [5], Timothy Nguyen [6], Victoria Piunova

IBM Almaden Research Center, 650 Harry Rd, San Jose CA 95120, USA

ARTICLE INFO

Article history:
Received 1 July 2015
Received in revised form
29 September 2015
Accepted 2 October 2015
Available online 9 October 2015

Keywords:
Water soluble nanogel core star polymers
Unimolecular micelles
Pyrene environmental probe
Encapsulation environment
Modeling and simulation

ABSTRACT

Star polymers with a crosslinked nanogel core constitute an unusual class of polymers with many arms emanating from the functionalized core. Although the core is usually hydrophobic, the arms can be hydrophobic, hydrophilic or amphiphilic. We describe the synthesis of biodegradable nanogel core stars which are largely water soluble and use encapsulated pyrene fluorescence to probe the environment both in aqueous solution and in solid thin films. In spite of the expected hydrophobic nature of the inner portions, the encapsulated pyrene environment seems quite polar. Although the molecular environment based on the pyrene fluorescent probe of the inner aliphatic polyester regions is more polar than expected for an aliphatic polyester, the molecular environment of the encapsulated probe in aqueous solution is influenced by the proximity of water even though simulations suggest that water excursions into the inner regions of the hydrophobic core area are rare and transient. NMR studies in water show the disappearance of the arm polyester signals. This and the pyrene environmental probe studies are consistent with collapse of the inner polyester regions and localization of the probe at or near the hydrophobic/hydrophilic interface as suggested in the simulations. This study has implications for the encapsulation of strongly hydrophobic cargos barring some loosening of the collapsed core by sterically-demanding substituents, increased hydrophobicity and/or some optimized specific interactions of the cargo with the core.

1. Introduction

Many therapeutic drugs and food supplements are quite hydrophobic and require a delivery vehicle for application in aqueous solution. Increasingly, these agents are nanostructured and often include nanoparticle-like entities such as lipid-based systems [1], dynamic micelles, covalently crosslinked or non-covalently stabilized micelles [2], polar and nonpolar polymeric nanoparticles [1a,d,3] which can be either biodegradable or not, inorganic nanoparticles including ceramic, semiconductor, metallic nanoparticles both magnetic and non-magnetic [4], etc. We and others have been studying a class of materials, which we describe as nanogel core star polymers [5] that have a small crosslinked core from which arms and other functionality protrude. Some of these materials are amphiphilic, unimolecular micelles with a small hydrophobic internal core which is crosslinked, often an additional hydrophobic section provided by the arms as well and an outer corona which is polar to interact with the aqueous environment and stabilize the particle in water. The result is a unimolecular micelle that is not in traditional dynamic equilibrium with its components, has no critical micelle concentration and is hence stable to extreme dilution. These structures can be biostable, biodegradable or biocompatible depending on the components of

* Corresponding author.
E-mail address: rdmiller@us.ibm.com (R.D. Miller).
[1] Faculty of Pharmacy, UiTM Puncak Alam Campus, 43600 Bandar Puncak Alam, Selangor, Malaysia.
[2] Department of Chemistry, Columbia University, MC 3178, 3000 Broadway New York NY 10027.
[3] Department of Physics and Astronomy, University of British Columbia, Vancouver British Columbia, Canada.
[4] Deceased.
[5] Koch Institute for Integrative Cancer Research, Massachusetts Institute of Technology, 500 Main St., Cambridge MA 02139.
[6] Gilead Sciences Inc., 333 Lakeside Dr, Foster City CA 94404-1147.

http://dx.doi.org/10.1016/j.polymer.2015.10.008
0032-3861/

the core and arms. We have previously reported the synthesis and encapsulation capabilities of polystyrene-based nanogel core based amphiphiles [5a] and we and others have reported the synthesis of biodegradable aliphatic polyester structures [5b,h,i] with this architecture. The polylactone biodegradable nanogel core stars reported previously by ring opening polymerization were not water soluble and hence limited in their potential biomedical applications. Here we report the synthesis and characterization of water soluble, biodegradable nanogel core polylactone stars by organic-catalyzed ring opening polymerization and probe the nature of the interior hydrophobic cargo space using environmental spectroscopic probes. Earlier computational studies on smaller related unimolecular, amphiphilic model particles [6] suggested that in aqueous solution the inner hydrophobic portions of the arms collapsed into a dense extended core that could be described as either crystalline or glassy depending on the substituents with little water penetration and very short water residence time for water molecules that do visit [6b]. The extent of densification depends on among, other things, the nature of the hydrophobic arms (i.e. densification decreases in going from poly(ethylene), to poly(lactide) to poly(valerolactone). Shape analysis suggested an extended hydrophobic core which is almost fractal-like with many nooks and crannies so that water can get relatively close to the core section without actually penetrating and a sharp boundary between the hydrophobic and hydrophilic portions of the particle (i.e. phase separation). On the basis of these simulations, it was suggested that a hydrophobic cargo without a strong affinity for the extended core [2a,6b,7] might have trouble penetrating the dense, glassy core region and could reside on the surface at the hydrophilic–hydrophobic interface. Such a situation could have strong consequences for both drug loading levels and delivery which is facilitated by aqueous contact and/or the hydrolytic/enzymatic degradation of the polyester arms/core. Here we show the collapse of the hydrophobic portions in water by NMR and use the encapsulated hydrophobic environmental spectroscopic probe pyrene to probe the molecular interior. The results of the latter suggest cargo location at or near the hydrophobic–hydrophilic interface, consistent with computational predictions. The two polymer structures studied both had cross-linked caprolactone-like nanogel inner cores. In the case of structure **1,** the arms were composed of poly(ethylene glycol) (PEG) only while in structure **2** the arms were composed of a linear block copolymer comprised of PEG and poly(valerolactone) (PVL) blocks. Both the collapsed, densified structure and the cargo confinement near the phase separated interface could have consequences for cargo loading.

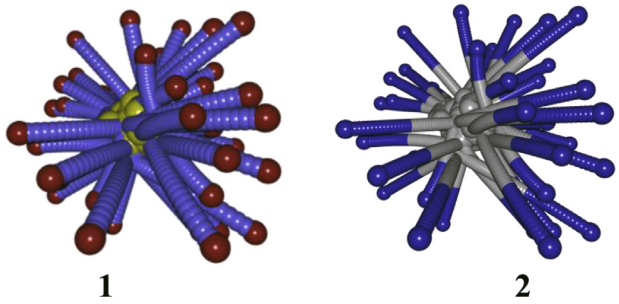

2. Experimental

^{1}H NMR spectra were recorded on a Bruker Avance 2000 spectrometer operating at 400 MHz (proton) and were referenced to internal solvent ($CDCl_3$, ^{1}H = 7.26 ppm). All NMR spectra were recorded at room temperature using standard Bruker library pulse programs. All chemicals and solvents were purchased from Aldrich Chemical Co (Milwaukee, WI), unless stated otherwise. Solvents were ACS reagent grade and the 1,5,7-triazabicyclo [4.4.0] dec-5-ene (TBD) was purim grade (>98%). Deuterated solvents were purchased from Cambridge Isotopes (Andover MA) and used as received. 4, 4′ − Bicyclohexanone was supplied by TCI America (>98%) and was used as received, α-methoxy-ω-hydroxy terminated poly(ethylene oxide) (PEO-OH) (*M*n ~ 5 kDa, PDI = 1.02) was obtained from Fluka/Sigma–Aldrich, purified by azeotropic distillation using benzene and dried under vacuum prior to use, δ-valerolactone (VL, technical grade) was purified by vacuum distillation from calcium hydride. 1,5,7-Triazabicyclo[4.4.0]dec-5-ene (TBD) was purified by sublimation before use. Bis-ε-caprolactone (BOD) was prepared from 4, 4′ − bicyclohexanone according to earlier published procedure (vide infra) [5h]. Anhydrous toluene, benzoic acid and diethyl ether were used as received.

Analytical gel permeation chromatography (GPC) was performed in THF using Waters high resolution columns HR1, HR2, HR4E and HR5E (flow rates 1 mL/min) and peaks detected using either a Waters 996 diode array or a Waters 411 differential refractometer and calibrated polystyrene standards to determine molecular weights and polydispersities. Dynamic Light Scattering (DLS) measurements yielded values for Mw, Mw/Mn and hydrodynamic radii (R_H) using the described GPC column set with a Wyatt DAWN EOS multi-angle light scattering detector. Differential Scanning Calorimetry (DSC) was performed with a TA Instruments Q1000 calorimeter heating at 5° C/minute. UV–vis spectra were recorded at room temperature using an Agilent UV–vis spectrometer (8453) with a diode array detector. The fluorescence spectra, both in solution and as solid films, were recorded at right angle geometries on a Horiba Scientific Fluorolog fluorescence spectrometer. Emission spectra were collected using 1 cm path length quartz cuvettes for solutions and 1 inch quartz disks for the films at a slit width of 1 nm. For the solution fluorescence measurements, the absorbance of the solution was adjusted to <0.2 at the excitation wavelength (usually 310–320 nm). The emission spectra were scanned from 365 to 500 nm with a slit width of 1 nm.

2.1. Materials and methods

2.1.1. Synthesis of PVL-PEO arms

In a glove box, to a solution of hydroxy-terminated poly(-ethylene oxide) arms (2 g, 0.4 mmol) (molecular weight 5 kDa) and TBD (8.65 mg, 62.2 μmol) in 7 g of dry toluene a solution of VL (1.2 g, 12.0 mmol) in 2.5 g of dry toluene ([VL]/[PEO-OH] = 30) was added with stirring. The mixture was allowed to react at room temperature for 30 min and then the polymerization was terminated by precipitation from 100 mL of cold diethyl ether. The resulted polymer was filtered and dried under vacuum at room temperature for 24 h. White amorphous powder (2.1 g, 68%). ^{1}H NMR ($CDCl_3$, 400 MHz): δ (ppm) = 4.09 (tr, 57H, $-CH_2-\mathit{CH_2}-OOC-$), 3.66 (br, 452H, $-O-\mathit{CH_2}-\mathit{CH_2}-O-$), 3.39 (s, 3H $-OCH_3$), 2.35 (tr, 59H, $-CH_2-\mathit{CH_2}-COO-$), 1.70 (br, 112H, $-OOC-CH_2-\mathit{CH_2}-\mathit{CH_2}-CH_2-OOC-$). GPC (RI): Mn_{GPC} (PDI) = 9.8 kDa (1.08), Mw = 10.6 kDa, R_H in THF = 7.8 nm, Mn ^{1}H NMR = 7.85 kDa. From the NMR, the molecular weight of the PVL block was determined to be 2.85 kDa based on a 5 kDa macroinitiator segment.

2.1.2. Synthesis of star polymer with PVL-PEO arms (2)

In a glove box, to a solution of PVL-POE-OH arms (0.864 g, 0.11 mmol) in 5.5 g of anhydrous toluene, bis-ε-caprolactone (BOD) (0.84 mmol, 0.19 g) was added, followed by addition of 0.1 g of 5wt% solution of TBD in toluene. The reaction mixture was allowed to stir at 35 °C. After 16 h the reaction was quenched with 20 mg of

benzoic acid and resulting solution was precipitated from cold diethyl ether. The obtained precipitate was filtered and dried at room temperature. The crude polymer was dissolved in 4 mL of DCM and 18 mL of diethyl ether was slowly added to a stirred solution. The resulting emulsion was allowed to settle for 5 h, forming transparent oil at the bottom of the flask. The solution was decanted off and the oil was dissolved in a minimum amount of DCM, precipitated from ethyl ether, filtered and dried under vacuum for 24 h. White amorphous powder (0.48 g, 56%). ^{1}H NMR: ($CDCl_3$, 400 MHz): δ (ppm) = 4.09 (br, 84H, $-CH_2-CH_2-OOC-$), 3.66 (br, 452H, $-O-CH_2-CH_2-O-$), 3.39 (s, 3H $-OCH_3$), 2.35 (tr, 84H, $-CH_2-CH_2-COO-$), 1.70 (br, 160H, $-OOC-CH_2-CH_2-CH_2-CH_2-OOC-$). GPC (RI): Mn (PDI) = 69.2 kDa (1.20), R_H (THF) = 14.9 nm, Mw (LS, THF) = 219.3 kDa, average number of arms (ANA) = 28.

2.1.3. Synthesis of star polymer with PEO arms (1)

In a glove box, to a solution of poly(ethylene oxide) arms (0.11 mmol, 0.55 g) (molecular weight 5 K) in 5.5 g of anhydrous toluene, bis-ε-caprolactone (BOD) (0.84 mmol, 0.19 g) was added, followed by addition of 0.1 g of 5 wt.% solution of TBD in toluene. The reaction mixture was allowed to stir at 35 °C. After 16 h the reaction was quenched with 20 mg of benzoic acid and resulted solution was precipitated from cold diethyl ether. Obtained precipitate was filtered and dried at room temperature. The crude polymer was dissolved in 3 mL of DCM and 15 mL of diethyl ether was slowly added to a stirred solution. Resulted emulsion was allowed to settle for 2 h, forming transparent oil at the bottom of the flask. The solution was decanted off and the oil was dissolved in a minimum amount of DCM, precipitated from ethyl ether, filtered and dried under vacuum for 24 h. White amorphous polymer, (0.29 g, 53%). ^{1}H NMR ($CDCl_3$, 400 MHz): δ (ppm) = 4.9–3.9 (br, 32H, $-CH_2-CH_2-OOC-$), 3.58 (br, 386H, $-O-CH_2-CH_2-O-$, from the core $-CH_2-OH$), 3.30 (s, 3H, $CH_3-O-CH2$), 2.9–2.1 (br, 30H, $-CH_2-CH_2-COO-$), 1.9–1.4 (br, 52H, $-OOC-CH_2-CH_2-CH_2-CH_2-OOC-$). GPC (RI): Mn(PDI) = 38.7 kDa (1.10), Mw = 42.6 kDa, R_H (THF) = 9.5 nm, Mw(LS, THF) = 70.3 kDa, AN = 14.

3. General procedure for encapsulating pyrene into nanogel core star polymers

20 mg of the nanogel core star polymer(s) were weighed into a vial with amounts of purified pyrene ranging in amounts from 1 to 5 wt.% based on solids. The solids were dissolved in 300–400 μL of THF or acetone where all of the solids are dissolved. The mixture is stirred magnetically and 2 mL of MilliQ water was added dropwise. After stirring for 1 h at room temperature the residual organic solvent was evaporated by sparging, the solutions were filtered through a 0.45 μm Nylon filter and the clear solutions used for the spectroscopic studies.

4. Polymer films containing pyrene

Approximately 100 mg of polystyrene (Mn = 275 kDa), poly(-caprolactone (Mn = 45 kDa) and poly(methyl methacrylate), (Mn = 50 kDa) were dissolved in 2 mL of toluene, ethyl acetate and methyl ethyl ketone respectively. To each of these solutions were added ~1.0–5.0 mg of solid pyrene and the solutions stirred at room temperature for 8 h. The solutions were filtered through a 0.45 micron Teflon filter and used for the preparation of the films studied. The films were prepared by spinning the respective solutions at 2000 rpm for 30 s and the resulting films were dried at room temperature overnight. The fluorescence spectra were measured at 310 nm excitation and scanned from 365 to 500 nm. The $\mathbf{I_1/I_3}$ emission ratios were 1.07 for the PS, 1.47 for the linear PCL sample and 1.38 for the PMMA sample.

5. Preparation of micellar solutions from PEG-PVL linear arms

20 mg of the linear block copolymer used to prepare the nanogel core star **2** were dissolved in 400 μL of THF. The solution was diluted with stirring with 2 mL of distilled water and the organic solvent removed by sparging in a nitrogen stream directed above the sample. The process was stopped when 150% by weight of the added THF had been removed and the solution was filtered through a 0.45 μm Nylon filter. The R_H of the micelles in this solution was ~29 nm. Some larger aggregates were removed by filtration. The pyrene encapsulated by the micellar solution was prepared in the same fashion except ~0.2–0.4 mg of pyrene was added to the solid polymer before dissolution in THF.

6. Results and discussion

The nanogels stars **1** and **2** were prepared using the corresponding MeO-PEG (m-PEG) macroinitiator (5 kDa, OH terminated) using a basic organic catalyst (TBD) and the bis-lactone crosslinking reagent (BOD). Controlling the stoichiometry of the reagents allows some control of the size and molecular weight of the nanogel stars. The GPC traces of both the hydroxyl functionalized linear block copolymer (PEG-PVL-OH) and the corresponding nanogel star are shown in Fig. 1.

Fig. 2 shows the ^{1}H NMR spectra of the nanogel core star **2** where the arms are comprised of a linear block copolymer of PEG and poly(valerolactone) in a good solvent (a) for both blocks ($CDCl_3$) and (b) in a good solvent for PEG (H_2O) but a poor solvent for poly(valerolactone). In all of the nanogel stars studied, the inner most crosslinked core derived from the BOD was not detected because of the broadening of these signals. The collapse of the inner arms in water is obvious while the PEG corona remains extended in both solvents as shown in Fig. 2. While water is a good solvent for the PEG portion, it is a very poor solvent for the poly(valerolactone) portion and presumably also the crosslinked core portions of the star as well, leading to extensive broadening of these signals in the in the NMR spectra. As expected, the signals for the PEG portion including the methoxy end group at δ = 3.24 appear relatively unaffected in both solvents. The ^{1}NMR studies are consistent with a collapsed inner core as predicted by the simulations. Although the

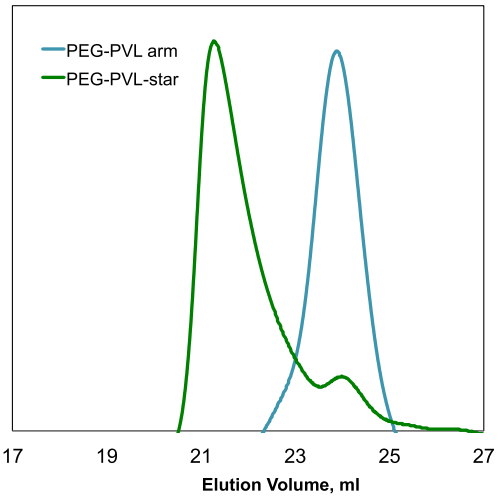

Fig. 1. GPC traces of linear block copolymer arms (PEG-PVL) and the nanogel star **2** derived from these arms by coupling with BOD using an organic catalyst.

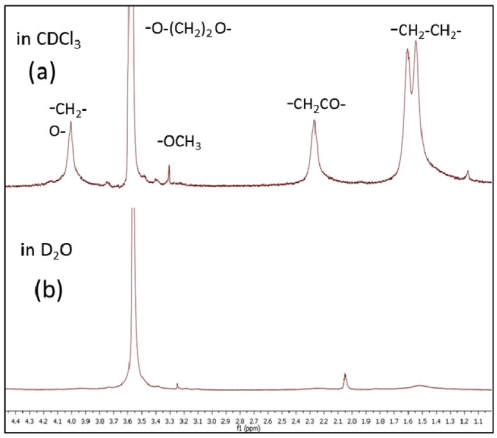

Fig. 2. ^{1}H NMR spectra of **2** in (a) $CDCl_3$ and (b) in D_2O.

measured hydrodynamic radius of **2** in water was relatively constant over the measured concentration range (0.6–5 wt.%), the question of aggregation in aqueous solution over time remains open, suggesting an opportunity for solution SAXS/SANS studies in the future.

While the NMR studies verify the hydrophobic collapse, the important question of cargo distribution in the hydrophobic region remains. There are a number of ways reported to probe the encapsulation environment using spectroscopic probes. The use of solvatochromic dyes is one approach, assuming that the dye is soluble in the nanostructure and not very soluble in the surrounding media [8]. For these studies, shifts in the UV–vis spectra of the probes are produced either by solvatochromism of the monomer or by aggregate formation. Solvatochromic dyes have also been used to probe the interior environment of dynamic micelles [9]. Another common probe is pyrene where the ratio of the first and third vibronic emission bands responds dramatically to the pyrene environment [10]. In such cases, the I_3 band is relatively insensitive to polarity while the I_1 band is much more so. This technique has also been used to study the critical micelle concentration in dynamically assembling systems [11]. As a result of these extensive studies of solvent effects on the nature of the pyrene emission, an empirical solvent polarity scale (Py) has been developed and tested. The parameter employed for the development of the Py scale is the $\mathbf{I_1/I_3}$ ratio of the first and third vibronic bands in the emission spectra. The solvent characteristics for more than 95 solvents have been mapped using this emission parameter. The vibronic structure in the absorption spectrum (ratio of measured extinction coefficients) has also been used to predict polarity, albeit less frequently [10a]. We note that reported $\mathbf{I_1/I_3}$ values for the Py solvent scale range from ~0.5 for fluorocarbons and saturated hydrocarbons to ~1.9 for water itself. The only measured solvent with a higher Py than water is DMSO with a value of 1.95.

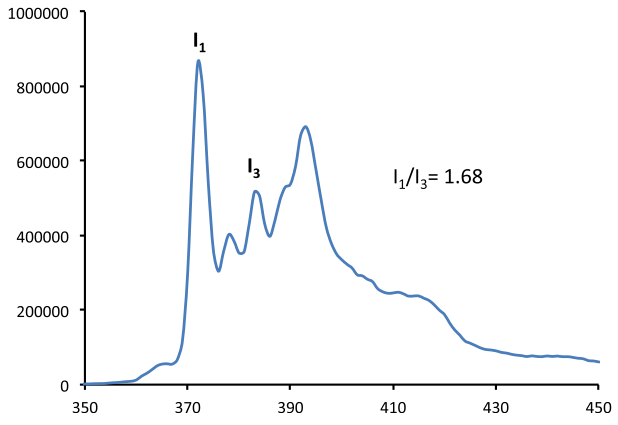

Fig. 3. Fluorescence spectrum of pyrene encapsulated in the nanogel star polymer **2** recorded in water; I_1 and I_3 emission bands are labeled on the Figure.

The Py values measured from pyrene emission have also been empirically correlated with the common E_T polarity scale which has been assembled from the solvatochromism of a variety of betaine dyes and has been described in detail by Reichardt et al. [8a,12]. Correlation of the Py values with known E_T values by regression analysis gives two series, one for protic and one for aprotic solvents [10d]. Solvatochromic studies have also been used to probe the micropolarity of micelles as a function of structure and the results used to predict the extent of water penetration into the hydrophobic core [10b]. Since we are studying solvent effects primarily in water, the equation for the conversion of the Py scale to E_T values in protic solvents is most appropriate and is shown below.

$$Py = 0.0584\,E_T - 1.75 \quad (1)$$

The absorption and emission spectrum of pyrene encapsulated in the nanogel core star polymer **2** is shown below (Fig. 3) and the I_1 and I_3 emission bands of interest are labeled. The measured hydrodynamic radii of **2** in water are very similar both in the presence and absence of pyrene (13.5 vs 12.3 nm respectively). This eliminates the possibility of formation of some amphiphilic, multimolecular aggregate in the presence of pyrene. The $\mathbf{I_1/I_3}$ ratios for pyrene encapsulated in the two biodegradable star polymer dissolved in water are 1.61 for star **1** and 1.68 for star polymer **2**. The values for the two polymers are quite similar as expected given the similarity of the polymer structures.

The first observation is that the Py values of the encapsulated pyrene in water are quite high, although not nearly as high as for water itself. Protic solvents with comparable values on the Py scale are quite polar with representative examples such as glycerol, ethylene glycol, acetone and glymes. Conversion of the measured Py values to the corresponding solvatochromic E_T values using Eq. (1) gives values of 57.53 for nanogel star **1** and 58.73 for nanogel star **2**. Comparison with the solvent parameter table for hydrogen bonding solvents (Table 1) would suggest a polarity environment in the stars, which is similar to 1-propanol (58.7) and somewhat less polar than ethanol (60.6). By either comparison, the pyrene environment is much more polar than expected if the pyrene were buried in the relatively less polar PVL-PCL region of the molecule (vide infra). Whatever the technique, the values of the pyrene solvent parameters in the polymer encapsulated form would

Table 1
Calculated E_T values (Eq. (1)) for pyrene encapsulated in the nanogel stars **1** and **2** in water in comparison with selected known E_T values for certain hydrogen bonding solvents.

Solvent (HB)	ET value
Morpholine	47.7
PEG-PCL-c/Py	57.5
1-Butanol	57.8
1-Propanol	58.7
PEG-PVL-PCL-c/Py	58.7
Ethanol	60.6
N-Methylformamide	63.1
Methanol	64.6
Water	70.2

suggest that there is a significant amount of water in the vicinity of the probe, a conclusion which is unexpected if the pyrene was buried deep in the PVL-c-PCL region of the polymer where computation suggests that water visits infrequently with a very short residence time.

As mentioned, pyrene encapsulation has also been used to probe the interior environment of dynamic micelles formed from typical small molecule surfactants. Kalyanasundaran and Thomas studied the spectroscopy of pyrene encapsulated in a variety of small molecule surfactants including anionic, cationic and nonionic examples and found $\mathbf{I_1/I_3}$ values ranging from 1.04 to 1.37 with the largest values occurring for the cationic surfactants [10b]. Their conclusion was that the interior of the micelle is not truly hydrophobic as expected for an alkane and water must penetrate to the interior, with the greatest effective penetration occurring for components with large head groups which form somewhat disordered micelles. Our measured values of $\mathbf{I_1/I_3}$ for the nanogel star polymers (1.61–1.68) are much larger than the micellar values reported by Kalyanasundaran and Thomas [10b]. There are a number of possible reasons for the higher values observed for the star polymers. Assuming that the micellar values truly reflect the polarity of the encapsulated environment, that of the small molecule micelles studied should be hydrocarbon-like while the environment of the hydrophobic portion of nanogel stars (**1** and **2**) should be more like poly(valerolactone) or poly(caprolactone). Although intuitively this environment should be significantly less polar than the PEG portion because of the presence of the bridging methylene chains, the simulations have shown that the interactions between the ester functionalities are significant [6b] and are partially responsible for the exclusion of water from the collapsed polyester cores in the nanogel stars (vide infra). It is tempting to conclude that the lower values reported for the dynamic micelles could be attributed to the combination of the fact that they are essentially small molecules with rapid diffusion and the tails are all hydrocarbon-like. A question remains regarding the intrinsic polarity of poly(valero or caprolactone) segments. We have also studied the emission of pyrene incorporated in low concentrations into a variety of polymer films with no water present and have measured the respective $\mathbf{I_1/I_3}$ values. Although no comprehensive list of $\mathbf{I_1/I_3}$ values for pyrene in polymers exits, as in the case of small molecule solvents, to allow quantitative assessment of the microenvironment, we and others [13] have noticed that the $\mathbf{I_1/I_3}$ values increase as expected with polarity for the small number of polymers that have been surveyed e.g.(poly(styrene)-1.07, poly(methyl methacrylate) −1.39, poly(vinylpyridine)-1.49 etc. As expected the vibronic ratios were significantly larger in polyvinylpridine (1.49) than in polystyrene (1.05) and $\mathbf{I_1/I_3}$ values have been used to predict the location of pyrene dissolved in phase-separated block copolymers [13]. For comparison, our values measured for polystyrene were very similar to those reported in the literature (1.07 vs 1.05). Interestingly and perhaps fortuitously, the numbers measured for pyrene in the pure polymers mimic those of solvent values with similar structures to the respective polymer side chain: polystyrene-benzene/toluene- 1.0, PMMA-ethyl acetate- 1.37, polyvinyl pyridine-pyridine- 1.42 etc. Finding an appropriate solvent model for the respective polymers from published data is not always easy. When the $\mathbf{I_1/I_3}$ value of pyrene incorporated into polycaprolactone (~1 wt.%) was measured, it was surprisingly high (1.47). For these measurements, the concentration of the pyrene was deliberately kept low to minimize the formation of pyrene excimer with a broad emission maximum ~475 nm which can complicate the $\mathbf{I_1//I_3}$ analysis of monomeric pyrene. Consistently, the $\mathbf{I_1/I_3}$ value for pyrene encapsulated in a star polymer such as **2** but without the PEG corona was 1.45, a value similar to that in linear PCL itself. . The $\mathbf{I_1/I_3}$ ratio of pyrene encapsulated in the dry star polymer **1** film was 1.46 while the value in the nanogel star **2** was slightly higher at 1.49. For comparison, the ratio for pyrene dissolved in dry 5 K PEG was significantly higher at 1.66. The lower ratios for the nanogel star films dry, suggest that the higher values measured in aqueous solution result from proximity to solvating water. Clearly, the $\mathbf{I_1/I_3}$ ratios measured for the nanogel stars in water are higher than expected if the pyrene probe was buried deep in the polyester core. The unexpectedly polar environment for an aliphatic polyester predicted by the fluorescence studies is consistent with the presence and interaction of polar chain carbonyl functionality as predicted earlier by computation [6b] which showed that the carbonyl groups have an effective charge distribution that promotes significant electrostatic interactions. This carbonyl interaction in fact is proposed to be more favorable than the water–carbonyl interactions in aqueous solutions resulting in collapse of the poly(valerolactone) arms and phase separation of the PEG-PVL stars in aqueous solution. The relatively high value of $\mathbf{I_1/I_3}$ measured for pyrene in polycaprolactone films leads to the surprising conclusion that PCL even in the absence of water appears to be more polar than expected for a polymer with five methylene groups/monomer unit which provide both flexibility and hydrophobicity. This could have implications for loading highly lipophobic materials into PCL domains in aqueous solution. The measured $\mathbf{I_1/I_3}$ values for the nanogel star polymers **1** and **2** in aqueous solution are substantially higher than for PCL films suggesting that the environment of the probe is influenced by the water solvent.

As discussed, the elevated $\mathbf{I_1/I_3}$ ratios observed in aqueous solutions involve interaction of pyrene with water, which modifies the environment. Since the numbers reported for pyrene in small molecule micelles were all <1.4 and sometimes substantially so, we measured the respective $\mathbf{I_1/I_3}$ values in an aqueous micellar solution generated from a linear block copolymer composed of PEG and poly(valerolactone). This block copolymer had the same composition as the arms in the nanogel star **2**. Aqueous solutions were prepared at 1wt. % of polymer to water and dynamic light scattering showed an R_H of ~30 nm for the linear polymeric micelle measured by DLS. The pyrene (1 wt. % based on solids) vibronic ratio in the micellar solution was 1.64, similar to that measured in the nanogel star polymers and substantially larger than reported for the smaller molecule micelles. This number is also similar to that previously reported for micelles derived from the linear polymer PCL 40-PEO 44 in water (1.68) [14a,b] and is substantially higher than reported for a number of other PEO-containing amphiphilic block copolymers containing more hydrophobic constituents e.g polystyrene-b-polyethylene oxide (1.2) [14c] and PBLA (polybenzyl aspartate -b-PEO- (1.41) [14d]. Since earlier measurements of the partition coefficients for pyrene and a PEO-PCL linear block copolymer micelle and water ranged from several hundred to a few thousand depending on the hydrophobic block length[13a], it would seem that most of the pyrene is associated with the more hydrophobic portion of the structure in aqueous solution.

Since the simulations [6,15] agree on the collapse of the inner blocks to a densified hydrophobic region into which water molecules make infrequent and very transient visits, a reasonable hypothesis is that the pyrene may be located at or near the hydrophobic–hydrophilic interface where it encounters transient water associated with the strongly solvated and mobile PEG block [6b]. Fig. 4 shows a typical snapshot for the simulation of a core-crosslinked star run at 400 K to speed the computation with an inner more hydrophobic section composed of poly(valerolactone) (translucent green), a typical polyester unit with a degree of polymerization of 8. The outer arms are PEG (red) and represent 6 PEG monomer units. The star studied computationally had 16 block copolymer arms based on an adamantane structural core. The core

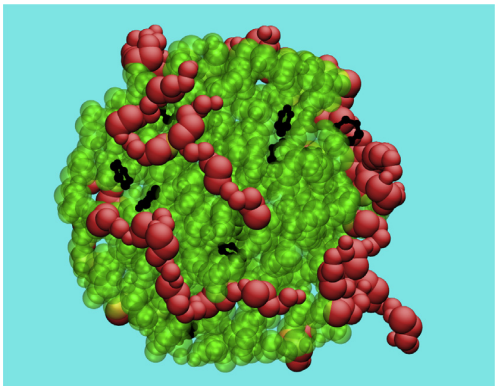

Fig. 4. Snapshot view of the simulation of the nanogel star polymer 2 (PEG-PVL c-PCL) in the presence of water (water molecules are removed for clarity: translucent green is PVL, red is PEG. 12 molecules of benzene (black) as a model hydrophobic cargo were added to the simulation is assess the landing preference. (For interpretation of the references to colour in this figure legend, the reader is referred to the web version of this article.)

in the simulations provided only a scaffold from which the linear arms emanated. The simulations were run in the presence of water hence the inner arms are collapsed and the PEG corona is somewhat more extended and is strongly associated with the water (water molecules of the simulation are deleted from Fig. 4 for clarity, see Supplemental Section). To probe the various intramolecular environments, 12 benzene molecules (black) were added to the simulation and their local environment studied (see supporting material for the simulation details). From the figure, you can see that the benzene molecules are more closely associated with the poly(valerolactone) section but not strongly buried. We define as buried when the molecule has little or no contact with water over time under the simulation conditions. The benzene molecules appear to be largely localized in the natural nooks and crannies of the hydrophobic portion of the star. Careful examination of the 3D picture from many views and under simulation conditions suggests that ~10% of the benzene molecules are buried in the collapsed hydrophobic portion of the molecule while the rest are localized at or near the hydrophobic–hydrophilic interface in a position where over time that they encounter water molecules. Although not simulated because of the molecular size, pyrene is substantially larger than benzene and one would expect further exclusion from the densified core in water. The PEG arms are strongly associated with water and are quite mobile, visiting the interface quite frequently. Examination of the simulation with the water present shows that there is no water in between the benzene molecule and the collapsed hydrophobic surface. Visits by water molecules to the interior of the hydrophobic core are infrequent and transient. The average environment of the benzene molecules can be roughly quantified by the percentage of the benzene surface associated with each of the components of the simulation i.e. ~70% associated with the hydrophobic portion of the molecule, 17% with water and 11% with the PEG (see Fig. S7 in the supplemental). From this analysis, it seems that the benzene is largely located at or near the hydrophobic–hydrophilic interface. The simulations also show that water is strongly associated with the PEG portion of the block copolymer arms, which appear quite mobile hence facilitating the interaction between water and any pyrene at the interfacial region of the nanogel star but probably not with the molecule in the densified hydrophobic interior. We point out that increasing the size of the PVL and the PEG units causes some changes in the details of the simulation but supports qualitatively similar conclusions [15]. This coupled with the experimental studies would strongly suggest that the encapsulation of very hydrophobic materials could reasonably be confined to nooks and crannies of the interfacial surface between the hydrophobic and hydrophilic portions of the nanogel stars, potentially limiting effective cargo loading.

7. Conclusions

We have described the versatile synthesis and characterization of water-soluble nanogel stars comprised of a biodegradable core and in one example an inner hydrophobic block. Earlier simulations suggested that such block copolymer structures would experience a collapse and densification of the hydrophobic portions of the arms in aqueous solution. NMR studies of such materials showed that this is the case. The environmental spectroscopic probe pyrene, when encapsulated into the nanogel stars, suggested a rather polar environment strongly influenced by water. This is also consistent with computational predictions that suggest that hydrophobic cargos lacking specific interactions in general would be confined to the peripheral interface between the collapsed hydrophobic core and the extended PEG arms providing the required transient contact with water. These studies lead to certain suggestions for how to improve the hydrophobic cargo loading in related systems. In particular, it would seem that alternative approaches to improved loading capacities could be the use of sterically demanding, hydrophobic inner cores that resist densification/crystallization upon collapse in an aqueous environment, tailoring specific interactions within the hydrophobic arms to the cargo (e.g. acid–base, hydrogen bonding, electrostatic, pi stacking etc) or by promoting solubility by matching respective polymer-cargo solubility parameters.

Acknowledgments

“This research is supported in part by NanoMalaysia Berhad, a Company Limited by Guarantee under the Ministry of Science, Technology and Innovation(MOSTI), and the Ministry of Education (MoE), Malaysia under a Joint Development Agreement between IBM Corporation and NanoMalaysia Berhad (Agreement No. A1360789)”. AJP also acknowledges partial funding from the MacDiarmid Institute for Advanced Materials and Nanotechnology, Wellington, New Zealand.

Appendix A. Supplementary data

Supplementary data related to this article can be found at http://dx.doi.org/10.1016/j.polymer.2015.10.008.

References

[1] a) Drug Delivery Nanoparticles Formulation and Characterization, in: Y. Pathak, D. Thassu (Eds.), Informa Healthcare, 2009 (New York NY);
b) J.Y. Fang, C.L. Fang, C.H. Liu, Eur. J. Pharm. Biopharm. 70 (2008) 633;
c) K.A. Shah, A.A. Date, M.D. Joshi, V.B. Patravale, Int. J. Pharm. 345 (1–2) (2007) 163, 124;
d) M.M. Gaspar, A. Cruz, A.G. Farga, A.G. Castro, M.E.M. Cruz, J. Pedrosa Curr. Top. Med. Chem. 19 (8) (2008) 579;
e) P. Couvreur, C. Vauthier, Pharm. Res. 23 (2006) 1417.
[2] a) C. Allen, D. Maysinger, A. Eisenberg, Colloids Surfaces B Biointerfaces 16 (1999) 3;
b) Y. Ohya, ACS Symposium Series (Tailored Polymer Architectures for Pharmaceutical and Biomedical Applications), 2013. Chapt. 7 Washington D.C;
c) L. Yu, L. Yao, J. You, Y. Gui, L.J. Yang, J. Appl. Polym. Sci. 131 (1) (2014), 39623/1;
d) K.B. Thurmond, T. Kowalewski, K.L.J. Wooley, Am. Chem. Soc. 118 (1996) 7239;
e) J.O. Kim, T. Ramasamg, C.S. Yong, N.V. Nukolora, T.K. Bronich, A. Kabanov, Mendeleev Commun. 23 (2013) 179;
f) Y. Shao, W. Huang, C. Shi, S.T. Atkinson, J. Luo, Ther. Deliv. 3 (12) (2012) 1409;
g) F. Nederberg, E. Appel, J.P. Tam, S.H. Kim, K. Fufushima, J. Sly, R.D. Miller,

R.M. Waymouth, Y.Y. Yang, J.L. Hedrick, Biomacromol 10 (6) (2009) 1460.
[3] a) T. Yoshikawa, N. Okada, A. Oda, et al., Biochem. Biophys. Res. Commun. 366 (2) (2008) 408;
b) P. Decuzzi, M. Ferrari, Biomater 29 (2008) 377;
c) J. Cheng, B.J.A. Teply, S. Ines, J. Sung, G. Luther, F.X. Gu, E. Levy-Nissenbaum, A.F. Radovic-Morenoz, R.S. Langer, O.C. Farokhzad, Biomater 28 (5) (2007) 869.
[4] a) T. Kim, T. Hyeon, Nanotechnology 25 (2014) 1;
b) R. Liang, M. Wei, D.G. Evans, X. Duan, Chem. Commun. 50 (91) (2014) 14071;
c) H. Mattoussi, V.M. Rotello, Adv. Drug. Del. Rev. 65 (5) (2013) 605.
[5] a) V.Y. Lee, K. Havenstrite, M. Tjio, M. McNeil, H.M. Blau, R.D. Miller, J. Sly, Adv. Mater. 23 (2011) 4509;
b) E.A. Appel, V.Y. Lee, T.T. Nguyen, M. McNeil, F. Nederberg, J.L. Hedrick, W.C. Swope, R.D. Miller, J. Sly, Chem. Commun. (2012) 6163;
c) J.G. Zilliox, P. Rempp, J. Parrod, J. Polym. Sci. A. Polym. Symp. 22 (1968) 145;
d) A. Sulistio, A. Blencowe, A. Widjaya, X. Zhang, G. Qiao, Polym. Chem. 3 (2012) 224;
e) J. Ferreira, J. Syrett, M. Whittaker, D. Haddleton, T.P. Davis, C. Boyer, Polym. Chem. 2 (2011) 1671;
f) A. Blencowe, J.F. Tan, T.K. Goh, G.G. Qiao, Polymer 50 (2009) 5;
g) J.T. Wiltshire, G.G. Qiao, Aust. J. Chem. 60 (10) (2007) 699;
h) J.T. Wiltshire, G.G. Qiao, Macromol 39 (13) (2006) 4282;
i) J.M. Ren, Q. Fu, A. Blencowe, G.G. Qiao, ACS Macro Lett. 1 (6) (2012) 681.
[6] a) L. Huynh, C. Neale, R. Pomes, C. Allen, Soft Matter 6 (2010) 5491;
b) W.C. Swope, A.C. Carr, A.J. Parker, J. Sly, R.D. Miller, J.E.J. Rice, Chem. Theory Comput. 8 (2012) 3733.
[7] a) R. Nagarajan, M. Barry, A. Ruckenstein, Langmuir 2 (1986) 210;
b) M. Tian, E. Arca, Z. Tuzor, E. Stephen, S.E. Webber, S.E. Munk, J. Polym. Sci. Part B Polym. Phys. 33 (1995) 1713.
[8] a) C. Reichardt, Chem. Rev. 94 (1994) 2319;
b) A.P. Demchenko, Y. Mely, G. Duportail, A.S. Klymchenko, Biophys. J. 96 (2009) 3461;
c) R. Varadaraj, J. Bock, P. Valint Jr., N. Brons, Langmuir 6 (1990) 1376;
d) J.F. Deye, T.A. Berger, Anal. Chem. 62 (1990) 615;
e) M.C.A. Stuart, J.C. van de Pas, J.B.F.N.J. Engberts, Phys. Org. Chem. 18 (2005) 929;
f) A.S. Klymchemko, Methods Enzym. 450 (2008) 37–58 (Fluorescence Spectroscopy).
[9] L.P. Novaki, O.A. El Seoud, Langmuir 16 (2000) 35.
[10] a) A.J. Nakajima, Mol. Spectrosc. 61 (1976) 467;
b) K. Kalyanasundaram, J.K.J. Thomas, Am. Chem. Soc. 99 (1977) 2039;
c) A. Nakajima, Bull. Chem. Soc. Jpn. 44 (1971) 3272;
d) D.C. Dong, M.A. Winnik, Can. J. Chem. 62 (1984) 2560.
[11] a) Wilhelm, M., Zhao, C.-L., Wang, Y., Xu, R., Winnik, M., Mura, J.-L., Reiss, G., Croucher, M.D. b) C.-L. Zhao, M.A. Winnik, G. Reiss, M.D. Croucher, Langmuir 6 (1990) 514;
c) J. Agular, P. Carpena, J.A. Molina-Bolivar, C. Carnero Ruiz, J. Colloids Interfaces 258 (1) (2003) 116;
d) A.V. Kabanov, I.R. Nazarova, I.V. Astafieva, E.V. Batrakova, V.Y. Alakhov, A.A. Yaroslovov, V.A. Kabanov, Macromol 28 (7) (1995) 2303.
[12] a) J.P. Ceron-Carrasco, D. Jacquemin, C. Laurence, A. Planchat, C. Reichardt, K.J. Sraidi, Phys. Org. Chem. 27 (2014), 512 12.
[13] K. Nakashima, M.A. Winnik, K.H. Dai, E.J. Kramer, J. Washiyama, Macromol 25 (1992) 6866.
[14] a) Thesis Jane Allen Christine, "Poly(caprolactone)-b-Poly(ethylene oxide) Copolymer Micelles: Physico-Chemical Characterization and Application in Drug Delivery" Department of Chemistry, McGill University, Montreal, Quebec Canada, September 1999;
b) C. Allen, D. Maysinger, A. Eisenberg, Colloids Surfaces B Biointerfaces 16 (1999) 3;
c) M. Wilhelm, C. Zhao, Y. Wang, R. Xu, M.A. Winnik, J.-L. Mura, G. Riess, M.D. Croucher, Macromol 24 (1991) 1033;
d) G. Kwon, M. Naito, M. Yokoyama, T. Okano, Y. Sakurai, K. Kataoka, Langmuir 9 (1993) 945.
[15] L.E. Felberg, D.H. Brookes, T. Head-Gordon, J.E. Rice, W.C. Swope, J. Phys. Chem. B 119 (2015) 944.